Published in final edited form as:
*Neuroradiology*. 2013 August ; 55(8): 1049–1056. doi:10.1007/s00234-013-1187-0.

# The Effects of Propofol on Cerebral Perfusion MRI in Children

**Julie H. Harreld**[a,*], **Kathleen J. Helton**[a], **Roland N. Kaddoum**[b], **Wilburn E. Reddick**[a], **Yimei Li**[c], **John O. Glass**[a], **Rakhee Sansgiri**[a], **Qing Ji**[a], **Tianshu Feng**[c], **Mary Edna Parish**[b], **Amar Gajjar**[d], and **Zoltan Patay**[a]

[a]Department of Radiological Sciences, St. Jude Children's Research Hospital, 262 Danny Thomas Place, Memphis, TN USA 38105-3678

[b]Department of Anesthesiology, St. Jude Children's Research Hospital, 262 Danny Thomas Place, Memphis, TN USA 38105-3678

[c]Department of Biostatistics, St. Jude Children's Research Hospital, 262 Danny Thomas Place, Memphis, TN USA 38105-3678

[d]Department of Oncology, St. Jude Children's Research Hospital, 262 Danny Thomas Place, Memphis, TN USA 38105-3678

## Abstract

**Introduction—**The effects of anesthesia are infrequently considered when interpreting pediatric perfusion MRI. The objectives of this study were to test for measurable differences in MR measures of cerebral blood flow (CBF) and cerebral blood volume (CBV) between non-sedated and propofol-sedated children, and to identify influential factors.

**Methods—**Supratentorial cortical CBF and CBV measured by dynamic susceptibility contrast perfusion MRI in 37 children (1.8–18 years) treated for infratentorial brain tumors receiving propofol (IV, n=19) or no sedation (NS, n=18) were compared between groups and correlated with age, hematocrit, end-tidal $CO_2$ ($ETCO_2$), dose, weight, and history of radiation therapy (RT). The model most predictive of CBF and CBV was identified by multiple linear regression.

**Results—**Anterior cerebral artery (ACA) and middle cerebral artery (MCA) territory CBF were significantly lower, and MCA territory CBV greater (p=0.03), in IV than NS patients (p=0.01, 0.04). The usual trend of decreasing CBF with age was reversed with propofol in ACA and MCA territories (r=0.53, r=0.47; p<0.05). ACA and MCA CBF (r=0.59, 0.49; p<0.05) and CBV in ACA, MCA and posterior cerebral artery (PCA) territories (r=0.73, 0.80, 0.52; p<0.05) increased with weight in propofol-sedated children, with no significant additional influence from age, $ETCO_2$, hematocrit, or RT.

**Conclusion—**In propofol-sedated children, usual age-related decreases in CBF were reversed, and increases in CBF and CBV were weight-dependent, not previously described. Weight-dependent increases in propofol clearance may diminish suppression of CBF and CBV. Prospective study is required to establish anesthetic-specific models of CBF and CBV in children.

### Keywords

magnetic resonance imaging; propofol; perfusion; pediatrics; brain

[*]Corresponding author at: Department of Radiological Sciences, MS 220, St. Jude Children's Research Hospital, 262 Danny Thomas Place, Memphis, TN 38105-3678. Telephone: + 1 901 595 4176. Fax: + 1 901 595 3981. julie.harreld@stjude.org (J. Harreld).

**Conflict of Interest**:
We declare that we have no conflict of interest.

## Introduction

In recent years, there has been increasing interest in developing quantitative cerebral blood volume (CBV) and cerebral blood flow (CBF) threshold criteria for evaluation of disease and treatment response [1–5]. Dynamic susceptibility contrast (DSC) perfusion magnetic resonance imaging (MRI), the most common technique currently in clinical use [6], relies on the measurement of T2* signal changes in a single volume of brain over time during the first pass of an intravenous (IV) contrast bolus and the identification of an arterial input function to approximate CBF, CBV, and mean transit time. Interpretation of perfusion data and the development of clinically useful quantitative thresholds are complicated by physiologic factors affecting cerebral perfusion, such as end-tidal $CO_2$ ($ETCO_2$) and hematocrit, which could introduce significant variability in a clinical setting [7, 8]. Interpretation of perfusion data in children is further complicated by age-related changes in CBF; it is well accepted that CBF decreases throughout childhood, reaching adult levels by the late teens [7, 9–12]. Particularly relevant to pediatric magnetic resonance (MR) perfusion imaging are the effects of anesthetic agents on cerebral perfusion, as a significant proportion of pediatric patients receive anesthesia for MRI.

Propofol, a sedative-hypnotic IV anesthetic agent commonly used in pediatric anesthesia, decreases CBF indirectly by decreasing the cerebral metabolic rate while preserving coupling with CBF and possibly by direct inhibition of vasodilatation by inhibition of vascular nitric oxide receptors [7, 8, 13]. Propofol-induced decreases in adult cortical CBF of up to 52% were observed in a recent dynamic 18F-FDG PET study [14]. CBV, which generally follows CBF, is also decreased by propofol, a property exploited in neurosurgical settings to decrease intracranial pressure [7]. Differences in propofol dose requirement due to age-related shifts in volumes of distribution and weight-dependence of propofol clearance could further complicate analysis of perfusion data in sedated children [15–17].

If not taken into account during data analysis, propofol-induced reductions in CBF and CBV could be falsely attributed to pathology. For example, if the CBF of a propofol-sedated child receiving brain irradiation were compared to the CBF of a non-irradiated, non-sedated child of the same age, a propofol-induced decrease in CBF in the sedated child could be erroneously attributed to radiation effects. Because young children are unlikely to be awake for MRI, a more common scenario in young children might involve comparing perfusion measures between a child receiving propofol and one receiving an inhalational halogenated agent such as sevoflurane or isoflurane, which increase CBF [18, 19], further exaggerating artificial differences in perfusion measures. Because reactivity of abnormal tumor vessels to anesthesia may not be the same as normal brain [19], ratio-based measures of tumor CBV for grading purposes may also be affected by anesthesia. Because “normal” age-related cerebral perfusion in children may depend on the agent administered, normative curves of pediatric cerebral perfusion could also be inaccurate if any subjects received anesthesia [10].

Accurate longitudinal or comparative analysis of DSC MR perfusion measures in children depends on whether anesthesia-induced alterations in CBF and CBV are evident, and, if so, clarification of these effects. We therefore performed a retrospective review of MR perfusion and anesthesia data collected in a clinical setting to test the hypothesis that propofol-induced alterations of CBF and CBV would be detectable by DSC perfusion imaging, and to characterize these effects in the context of other factors known to influence cerebral perfusion in children.

## Materials and Methods

### Subjects

Supratentorial DSC perfusion MRI data acquired in patients enrolled on either of two institutional prospective trials for patients with posterior fossa tumors were retrospectively reviewed, with institutional review board approval. Single examinations from 37 patients (46% male; mean age, 9.6 ± 5.2 years; range, 1.8–18 years) were analyzed, including 18 non-sedated (NS) patient exams (mean age, 14.2 years; range, 12–18 years) and 19 exams in patients sedated with IV propofol (mean age, 5.3 years; range, 1.8–11 years). All patients had undergone posterior fossa tumor resection (29 medulloblastomas, 3 atypical teratoid rhabdoid tumors, 3 anaplastic ependymomas, 1 high-grade glioma, and 1 pineoblastoma resected via posterior fossa approach) and had no current imaging or clinical evidence of residual, recurrent, or intracranial metastatic tumor. Twelve of 19 IV patients and all 18 NS patients received radiation therapy (RT). No patients received supratentorial high-dose RT; supratentorial dose ranged from 23.4 Gy to 39.6 Gy in both groups (mean, 28.0 ± 7 Gy for the IV group; mean, 25.7 ± 5.3 Gy for the NS group). All patients had undergone chemotherapy; no anti-vascular endothelial growth factor agents or routine steroids were given. Patients were excluded if systemic steroids had been given within 7 days before MRI (equivalent to 3.5 half lives and ~91% elimination of dexamethasone). Studies with visible brain parenchymal abnormalities or artifacts at the level of perfusion analysis (the “index slice,” Figure 1) were excluded. Hematocrit (Hct) was obtained within 4 days in all patients, on the day of MRI in 60%, within 1 day in 93%, and within 2 days in 97%. In the IV group, propofol was titrated to deep sedation, defined as the patient not being easily roused [20]; one IV patient was intubated for airway maintenance. All were spontaneously breathing. $ETCO_2$ was recorded for IV patients; because measurements were acquired via face mask probe, they were considered relative.

### MRI acquisition and processing

DSC perfusion MRI was performed at 1.5T (Magnetom Avanto, Siemens, Erlangen, Germany) before, during, and after the injection of 0.1 mmol/kg gadolinium-based contrast (Magnevist, Bayer HealthCare Pharmaceuticals, Wayne, NJ) followed by a 20 mL saline flush, with the following parameters: repetition time 1910 ms, echo time 50 ms, flip angle 90°, 15 slices, 4–5 mm slice thickness (no gap), 128 × 128 matrix, 1.6 mm × 1.6 mm in-plane voxel size, bandwidth of 1346 Hz/pixel (86.144 kHz). Because of variable vascular access, the contrast injection rate was standardized to 0.8–1 mL/s, tolerable by all devices. Perfusion data were randomized, anonymized, and transferred offline for analysis. Time-dependent contrast concentration C(t) was calculated from the T2* signal intensity by:

$$C(t) = -\frac{1}{TE} * Ln\left(\frac{S(t)}{S_0}\right)$$

where $S_0$ is the baseline intensity, $S(t)$ is the signal intensity over time and TE is the echo time for the imaging sequence. Following automated determination of the arterial input function (AIF) based on time concentration curves via an iterative Kohonen self-organizing map-based pattern recognition technique [21], the global AIF was used for nonparametric deconvolution by standard form Tikhonov regularization, a smooth version of truncated singular value decomposition (TSVD) [22]. The minimized generalized cross validation (GCV) technique was used to select the truncation threshold on a pixel-by-pixel basis [22, 23].

CBF was calculated as

$$CBF = \frac{k_H}{\rho} * \frac{C(t)}{\int_0^t C_a(\tau) R(t-\tau) d\tau}$$

and CBV is calculated as

$$CBV = \frac{k_H}{\rho} * \frac{\int C_t(t) dt}{\int C_a(t) dt}$$

where C(t) is the time-dependent contrast concentration, $C_a(t)$ is the AIF, $C_t(t)$ is the total concentration, $R(t-\tau)$ is the tissue residual function, $C_a(\tau)R(t-\tau)$ represents the fraction of contrast in the tissue at time $t$ after contrast injection at time $\tau$, and $k_H/\rho$ is a correction factor accounting for the difference in hematocrit between large vessels in which the AIF is measured and small vessels such as arterioles in the volume of interest ($k_H$), and the density of brain tissue ($\rho$) [24, 25]. CBV and CBF were scaled to units of mL/100g and CBF to mL/min/100g.

Gray matter (GM), white matter, and cerebrospinal fluid were segmented and color-coded according to an automated hybrid neural network segmentation and classification method using conventional clinical imaging sets of axial T1-weighted, T2-weighted, proton density, and fluid attenuation inversion recovery images [26, 27]. Perfusion images were co-registered to T2-weighted images using a normalized mutual information algorithm. Regions of interest corresponding to anterior cerebral artery (ACA), middle cerebral artery (MCA), and posterior cerebral artery (PCA) territories were manually delineated according to a standard vascular distribution map [28] (Figure 1). CBV and CBF were evaluated for cortical GM volumes by vascular territory.

### Statistical Analysis

Statistical analysis was performed using SAS, version 9.2 (SAS Institute, Cary, North Carolina). Pearson correlation coefficients were calculated to explore dependence of CBF and CBV by vascular territory on hematocrit, age, weight, raw and weight-adjusted propofol dose, and $ETCO_2$. Because not all patients had RT, the presence or absence of RT was also considered. Mean CBF and CBV by territory were compared between groups (Student's *t*-test) after verification of the normality of the data by Shapiro-Wilk test. Values for territorial CBF by age in the IV and NS groups were plotted against normative age-related cortical GM CBF as per Ogawa[11] ($\log Y = 2.26 - 0.29 \log X$, where Y = CBF and X = age in years) for qualitative comparison of age-related trends. Variables with a significant interaction with CBF, CBV, or both were incorporated into a multiple linear regression model to evaluate the relative contributions of each variable. The strongest regression models predicting CBF and CBV were selected based on the Bayesian information criterion (BIC).

## Results

### CBF by group and age

The IV group was significantly younger than the NS group ($p<0.0001$) but had significantly lower mean ACA and MCA territory CBF ($p=0.01$, 0.04) than the NS group. ACA and MCA territory CBF increased with age ($r=0.53$, $p=0.02$; $r=0.47$, $p=0.04$) in the IV group, contrary to age-related decreases in CBF in age-matched reference data (Figure 2); there was no significant correlation of age and PCA CBF.

In the NS group, there was no significant relationship between age and CBF; the slopes of the regression lines for territorial CBF by age did not differ significantly from 0 in the NS group (r=0.0007, −0.13, −0.13, p=1.0, 0.61, 0.59 for ACA CBF, MCA CBF, and PCA CBF, respectively) and followed a trend similar to age-matched reference data (Figure 2).

### CBV by group and age

MCA territory CBV was greater in the IV group than in the NS group (p=0.03). Relative increases in ACA and PCA territory CBV with IV compared with NS patients did not reach statistical significance. In the IV group, ACA and MCA CBV increased with age (r=0.56, p=0.01; r=0.67, p=0.002).

In NS patients, MCA CBV decreased with age (r=−0.48, p=0.04); decreases in CBV with age in the ACA and PCA territories did not reach statistical significance.

### Propofol dose

Propofol dose (mg/kg) decreased with age (r=−0.62, p=0.005). ACA and MCA CBV increased with decreasing propofol dose, (r=−0.55, −0.53; p=0.015, 0.019). Trends toward increasing PCA CBV and increasing CBF in all territories with decreasing dose were not statistically significant (PCA CBV: r=−0.34, p=0.15; ACA CBF: r=−0.39, p=0.10; MCA CBF: r=−0.25, p=0.30; PCA CBF: r=−0.09, p=0.72). Raw dose of propofol (mg) to titrate to deep sedation did not vary significantly with age or weight (r=0.15, 0.04; p=0.55, 0.87), and there was no significant correlation between raw dose and ACA, MCA or PCA territory CBF or CBV (CBF: r=0.16, 0.24, 0.12, p=0.51, 0.32, 0.63; CBV: r=0.003, 0.07, 0.01; p=0.99, 0.78, 0.97).

### Weight

Age and weight were strongly correlated in the IV group (r=0.90, p<0.0001). CBF and CBV in the ACA and MCA territories were more strongly correlated with weight than with age, and PCA CBV was moderately correlated with weight but not age (Table 2).

There was no significant correlation of age and weight in the NS group (p=0.11). ACA CBV decreased with increasing weight (r=−0.5211, p=0.027). Decreases in MCA and PCA CBV and CBF in all territories with increasing weight did not reach statistical significance (MCA CBV: p=0.14; PCA CBV: p=0.10; ACA CBF: p=0.22; MCA CBF: p=0.48; PCA CBF: p=0.23).

### Radiation therapy, $ETCO_2$, and hematocrit

IV patients who had RT (n=13) were older (p=0.0024), received a significantly lower propofol dose (p=0.04), and had greater ACA CBF (p=0.01) and ACA and MCA CBV (p=0.005, 0.004) than those who had not had RT (n=6). All NS patients had RT.

Relative $ETCO_2$, measured in the IV group only, was not significantly correlated with ACA, MCA or PCA territory CBF or CBV (CBF: p=0.56, 0.71, 0.32; CBV: p=0.46, 0.75, 0.50). Hematocrit was low in 58% of IV and 17% of NS patients, otherwise within the normal range for age. In the IV group, decreasing hematocrit was moderately correlated with increasing ACA and MCA CBV (r=−0.47, −0.50; p=0.04, 0.03), but was otherwise not significantly correlated with CBF or CBV. There was no significant correlation of CBF or CBV and hematocrit in NS patients.

Variables with a significant interaction with CBF or CBV in patients receiving IV propofol were thus identified as: age, weight, RT, and hematocrit. Multiple linear regression analysis with territorial CBF and CBV as the dependent variables and age, weight, hematocrit, and

RT (yes or no) as the independent variables was performed, with the best model determined by BIC. Weight was the only significant factor associated with CBV (ACA CBV p=0.0004, MCA CBV p<0.0001, and PCA CBV p=0.0231) and ACA and MCA CBF (p=0.0074, 0.0322) and was therefore the only independent variable in the final regression model (Table 3).

## Discussion

In this study, we found a reversal of the expected trend of decreasing CBF with age [7, 9–12] in patients receiving propofol for sedation at MRI and stronger positive correlations of CBF and CBV with weight than with age. As with models of propofol clearance, weight was the only significant determinant of CBV in all territories and anterior circulation (ACA and MCA) CBF in children receiving propofol, with no significant additional influence from age, hematocrit, or receipt of RT once weight was considered. This relationship was not present in NS patients, for whom age-related trends in CBF were similar to reference data.

Extensive study has established decreases in cerebral metabolic rate ($CMRO_2$), CBF and CBV with propofol [7, 8, 14, 29]. Though normative values of CBV in children have not been established to our knowledge, in the usual state CBV increases with increasing CBF [7]. Pharmacokinetic models show that propofol clearance increases with weight across all age ranges from neonate through adulthood, with no significant additional influence of age, sex, or duration of infusion [15–17]. It therefore stands to reason that CBF and CBV in patients sedated with propofol would increase as propofol clearance increases, resulting in decreased plasma propofol concentration and diminished inhibitory effects on $CMRO_2$ and vasodilatation. This is consistent with the rise in CBF and CBV with increasing weight we saw in our data. Because the central volume of distribution decreases with age in children, the per-kilogram dose required to achieve a given propofol plasma concentration also decreases with age [15]. Because weight and age are highly correlated in children, though not in a linear fashion [8], increases in CBF and CBV would be expected with both increasing age and weight, though the correlation with weight predominated in our series. Interestingly, only PCA territory CBF was not weight-dependent in this study. Technical or patient factors may contribute. With peripheral venous contrast administration, the arrival of the bolus to the PCA territory via the vertebrobasilar system would be expected to be delayed relative to the automatically-detected MCA AIF, potentially resulting in underestimation of PCA CBF, despite the relative delay-insensitivity of TSVD [6]. The shape of the AIF and tissue concentration curves in the PCA distribution also likely differed from that of the AIF, contributing to measurement error which could be reduced by using local AIFs in future studies. Undetected treatment effects, given the proximity of the vertebrobasilar PCA supply to the high-dose radiation field, could also be responsible.

The study of propofol clearance has presented challenges similar to those we face in studies of cerebral perfusion in children, including the necessity of considering colinearity of age and weight, maturation of metabolism, and changing volumes of drug distribution due to differences in body water content across age groups and differences in duration of drug infusion. However, multiple pharmacokinetic models considering these variables have shown weight to be the only significant influence on propofol clearance across all age ranges [15, 17]. These studies may serve as good models for the study of cerebral perfusion in children sedated with propofol, as we have shown here.

This study has several limitations. All NS children and some propofol-sedated children in this study received cranial radiation therapy, which induces microvascular changes. However, studies of perfusion of normal-appearing brain after RT in adults have found no definite evidence of significant perfusion alterations in normal brain receiving low-dose

radiation. In a study of 22 patients, a relative reduction in CBV of WM receiving >15Gy compared to <15Gy radiation was not statistically significant [30]. A study of 25 adults found decreased GM and WM CBV in adults after high-dose but not low-dose RT [31]. The level of the brain evaluated in our study was not in the high-dose field in any subject, and the presence or absence of prior RT did not prove to be a significant factor predicting CBF or CBV in our models. However, because these data were acquired in post-treatment brain, they cannot be considered normative, and prospective study in untreated, normal brain is required to establish anesthetic-specific models of CBF and CBV in children.

Because younger children cannot undergo MRI without anesthesia, and older children infrequently require it, there was too little overlap in age between IV and NS groups to perform statistically powerful age-matched comparison in this study. Because of age-related decreases in CBF with age in young children [7, 11, 32], direct comparison of CBF between children of different ages is not advised for clinical purposes. However, we perform this comparison to make the point that, contrary to CBF being greater in younger patients as expected, CBF in our younger, propofol-sedated group was *lower* than CBF in the older non-sedated group, significantly so in the ACA and MCA territories. This difference between groups, therefore, cannot be ascribed to expected age-related trends.

Adult studies have confirmed decreases in CBF of up to 52% with administration of propofol [14], but these findings are not directly translatable to young children, who demonstrate age-related differences in cerebral hemodynamics, anesthetic dose and response to anesthesia. Though a direct comparison of CBF and CBV in sedated versus non-sedated age-matched young children is theoretically appealing, the likelihood of a child between the ages of 1 and 8 undergoing MRI without sedation or anesthesia is extremely low; thus, such comparison is not practical in a clinical or research setting. To assess whether CBF and CBV truly deviate from normal in young children, it is therefore necessary to develop anesthetic-specific models of CBF and CBV in this age group. Because anesthesia-induced alterations may compromise normalization of tumor perfusion measures to normal-appearing brain [19], GM/WM ratios may prove to be more stable for purposes of comparison. However, GM/WM perfusion ratios have also been found to be age-related [10], and the utility of such a ratio requires prospective study.

CBF is maintained over the physiologic range of mean arterial pressure and partial pressure of oxygen in arterial blood, but is known to increase with increasing end-tidal $CO_2$ ($ETCO_2$) and with decreasing hematocrit [7, 8]. However, these relationships were not found in our study. Imprecise measurement of $ETCO_2$ via facemask probe due to mixing with supplemental oxygen may be partially responsible, as could propofol-related alterations in vascular $CO_2$ reactivity [19]. Measurements of hematocrit, though obtained within one day of MRI in 93% of patients in this study, would ideally be contemporaneous with MRI. Because capillary hematocrit is not easily obtained, we did not incorporate patient hematocrit into the perfusion calculation; rather, we chose to incorporate a constant accounting for the difference in hematocrit between large (AIF) and small (tissue) vessels [33]. Though this hematocrit ratio may change in ischemic states resulting in underestimation of CBF (by ~10% for a 30% increase in capillary hematocrit), this would not be expected to be a problem in this study, as no subjects had evidence of intracranial vascular stenosis or ischemia by conventional or diffusion-weighted imaging [6]. The cerebral small to large vessel hematocrit ratio has also been found to decrease with vasodilatation, which is inhibited by propofol [34]. Because propofol dose decreases, and clearance increases, with age, one would expect age-related increases in vasodilatation, decrease in hematocrit ratio, and decreasing CBF and CBV with age. This is opposite to the trends we observed, suggesting that the effects of propofol on cerebral perfusion, mediated by effects on both vasoreactivity and cerebral metabolic rate, outweigh the influence of

small changes in hematocrit ratio. Though age-related differences in hematocrit ratio may also exist, they have not been reported to our knowledge and the influence would also be expected to be small [25].

Because we prioritize a standardized contrast injection rate, we use a somewhat low rate of 0.8–1 mL/s, tolerated by all vascular access devices, potentially resulting in a decreased contrast-to-noise ratio, to which the TSVD algorithm is sensitive, increasing variability in perfusion measures [5, 22]. It has been suggested that partial volume influence on the AIF may cause overestimation of CBF and CBV [35]. Assuming that this effect would be greater in younger children with smaller vessel size, greater overestimates of CBF and CBV in younger children would decrease with age and increasing vessel size. The slope of such an age-related curve would be negative, opposite to the positive slope we found in propofol-sedated children in this study. It has actually been shown that partial volume effects on the AIF may lead to either overestimation or underestimation of the contrast agent concentration [36]. Thus, though both volume averaging and increased noise may increase the variability in the data, the error introduced would not be expected to skew the data in any particular direction. Despite this variability, the effect sizes in this study were large enough to detect statistical differences between groups with a relatively small sample size, and clear statistically significant relationships between CBV and CBF and weight were seen indicating that the sample size provides sufficient power for detection. It is expected that, with larger sample sizes and techniques promising more robust quantification such as ASL and bookend-technique DSC perfusion imaging, these effects will become increasingly apparent. Indeed, such effects have been noted, though not systematically investigated, in small numbers of children studied with ASL [10, 37]. It is therefore imperative for those interpreting or developing quantitative MR perfusion-based diagnostic criteria to understand and account for the effects of anesthetics on CBF and CBV, especially in children.

## Conclusion

In conclusion, expected age-related decreases in CBF were reversed in children sedated with propofol in this study. Weight was the only significant determinant of cortical GM CBV and CBF in children sedated with propofol for MRI, with no significant additional influence from age, hematocrit, or history of RT, a relationship not previously described and potentially related to weight-dependent changes in propofol clearance. These effects may obscure or mimic effects of treatment or disease. In children sedated with IV propofol, normalizing for weight may permit more precise perfusion-based characterization of brain tumors and their response to treatment; effects of treatment on normal brain; and perfusion effects of vasculopathy, with the caveat that abnormal vasculature in tumors or cerebrovascular disease may display differing reactivity to anesthetics, potentially rendering even ratio-based perfusion measures unreliable [4, 19, 38]. These effects will become increasingly important as the precision and utilization of quantitative MR perfusion measures evolves. This study establishes the need for prospective study establishing anesthetic-specific models of pediatric cerebral perfusion and clarifies the variables to be considered for accurate characterization of these effects.

## Acknowledgments

Supported in part by Grant No. CA21765 from the National Cancer Institute and by the American Lebanese Syrian Associated Charities.

## References

1. Hakyemez B, et al. High-grade and low-grade gliomas: differentiation by using perfusion MR imaging. Clin Radiol. 2005; 60(4):493–502. [PubMed: 15767107]

2. Tsien C, et al. Parametric response map as an imaging biomarker to distinguish progression from pseudoprogression in high-grade glioma. J Clin Oncol. 2010; 28(13):2293–2299. [PubMed: 20368564]
3. Lobel U, et al. Quantitative diffusion-weighted and dynamic susceptibility-weighted contrast-enhanced perfusion MR imaging analysis of T2 hypointense lesion components in pediatric diffuse intrinsic pontine glioma. AJNR Am J Neuroradiol. 2011; 32(2):315–322. [PubMed: 21087935]
4. Heiland S, Wick W, Bendszus M. Perfusion magnetic resonance imaging for parametric response maps in tumors: is it really that easy? J Clin Oncol. 2010; 28(29):e591. author reply e592. [PubMed: 20837945]
5. Salluzzi M, Frayne R, Smith MR. Is correction necessary when clinically determining quantitative cerebral perfusion parameters from multi-slice dynamic susceptibility contrast MR studies? Phys Med Biol. 2006; 51(2):407–424. [PubMed: 16394347]
6. Calamante F. Perfusion MRI using dynamic-susceptibility contrast MRI: quantification issues in patient studies. Top Magn Reson Imaging. 2010; 21(2):75–85. [PubMed: 21613873]
7. Miller RD, EL.; Fleisher, LA.; Wiener-Kronish, JP.; Young, WL. Miller's Anesthesia. 7th Edition. Vol. Vol.I. Elsevier, Inc.; 2010.
8. Szabo EZ, Luginbuehl I, Bissonnette B. Impact of anesthetic agents on cerebrovascular physiology in children. Paediatr Anaesth. 2009; 19(2):108–118. [PubMed: 19040505]
9. Barthel H, et al. Age-specific cerebral perfusion in 4- to 15-year-old children: a high-resolution brain SPET study using 99mTc-ECD. Eur J Nucl Med. 1997; 24(10):1245–1252. [PubMed: 9323265]
10. Biagi L, et al. Age dependence of cerebral perfusion assessed by magnetic resonance continuous arterial spin labeling. J Magn Reson Imaging. 2007; 25(4):696–702. [PubMed: 17279531]
11. Ogawa A, et al. Regional cerebral blood flow with age: changes in rCBF in childhood. Neurol Res. 1989; 11(3):173–176. [PubMed: 2573854]
12. Chiron C, et al. Changes in regional cerebral blood flow during brain maturation in children and adolescents. J Nucl Med. 1992; 33(5):696–703. [PubMed: 1569478]
13. Ogawa Y, et al. The different effects of midazolam and propofol sedation on dynamic cerebral autoregulation. Anesth Analg. 2010; 111(5):1279–1284. [PubMed: 20881283]
14. Schlunzen L, et al. Regional cerebral blood flow and glucose metabolism during propofol anaesthesia in healthy subjects studied with positron emission tomography. Acta Anaesthesiol Scand. 2012; 56(2):248–255. [PubMed: 22091956]
15. Rigby-Jones AE, Sneyd JR. Propofol and children--what we know and what we do not know. Paediatr Anaesth. 2011; 21(3):247–254. [PubMed: 21083787]
16. Shangguan WN, et al. Pharmacokinetics of a single bolus of propofol in chinese children of different ages. Anesthesiology. 2006; 104(1):27–32. [PubMed: 16394686]
17. Wang C, et al. A Bodyweight-Dependent Allometric Exponent for Scaling Clearance Across the Human Life-Span. Pharm Res. 2012
18. Matta BF, et al. Direct cerebral vasodilatory effects of sevoflurane and isoflurane. Anesthesiology. 1999; 91(3):677–680. [PubMed: 10485778]
19. Cenic A, et al. Cerebral blood volume and blood flow responses to hyperventilation in brain tumors during isoflurane or propofol anesthesia. Anesth Analg. 2002; 94(3):661–666. table of contents. [PubMed: 11867393]
20. Sury MR, Smith JH. Deep sedation and minimal anesthesia. Paediatr Anaesth. 2008; 18(1):18–24. [PubMed: 18095961]
21. Jain JJ, GJ.; Reddick, WE. SPIE International Symposium on Medical Imaging, Imaging Processing Conference. San Diego, CA: 2007. Automated arterial input function identification using self organized maps; p. 2-17.
22. Sourbron S, et al. Choice of the regularization parameter for perfusion quantification with MRI. Phys Med Biol. 2004; 49(14):3307–3324. [PubMed: 15357199]
23. Hansen CP. Reguarization Tools: A Matlab Package for Analysis and Solution of Discrete Ill-Posed Problems. Numerical Algorithms. 1994; 6(1):1–35.

24. Calamante F, et al. Measuring cerebral blood flow using magnetic resonance imaging techniques. J Cereb Blood Flow Metab. 1999; 19(7):701–735. [PubMed: 10413026]
25. Calamante F, Gadian DG, Connelly A. Quantification of perfusion using bolus tracking magnetic resonance imaging in stroke: assumptions, limitations, and potential implications for clinical use. Stroke. 2002; 33(4):1146–1151. [PubMed: 11935075]
26. Reddick WE, et al. Automated segmentation and classification of multispectral magnetic resonance images of brain using artificial neural networks. IEEE Trans Med Imaging. 1997; 16(6):911–918. [PubMed: 9533591]
27. Glass JO, et al. Improving the segmentation of therapy-induced leukoencephalopathy in children with acute lymphoblastic leukemia using a priori information and a gradient magnitude threshold. Magn Reson Med. 2004; 52(6):1336–1341. [PubMed: 15562471]
28. Blumenfeld, H. Neuroanatomy Through Clinical Cases. 2nd ed. Sinauer Associates, Inc; 2011.
29. Kaisti KK, et al. Effects of sevoflurane, propofol, and adjunct nitrous oxide on regional cerebral blood flow, oxygen consumption, and blood volume in humans. Anesthesiology. 2003; 99(3):603–613. [PubMed: 12960544]
30. Lee MC, et al. Dynamic susceptibility contrast perfusion imaging of radiation effects in normalappearing brain tissue: changes in the first-pass and recirculation phases. J Magn Reson Imaging. 2005; 21(6):683–693. [PubMed: 15906330]
31. Fuss M, et al. Radiation-induced regional cerebral blood volume (rCBV) changes in normal brain and low-grade astrocytomas: quantification and time and dose-dependent occurrence. Int J Radiat Oncol Biol Phys. 2000; 48(1):53–58. [PubMed: 10924971]
32. Leenders KL, et al. Cerebral blood flow, blood volume and oxygen utilization. Normal values and effect of age. Brain. 1990; 113(Pt 1):27–47. [PubMed: 2302536]
33. Rempp KA, et al. Quantification of regional cerebral blood flow and volume with dynamic susceptibility contrast-enhanced MR imaging. Radiology. 1994; 193(3):637–641. [PubMed: 7972800]
34. Sakai F, et al. Regional cerebral blood volume and hematocrit measured in normal human volunteers by single-photon emission computed tomography. J Cereb Blood Flow Metab. 1985; 5(2):207–213. [PubMed: 3921557]
35. Ziegelitz D, et al. Absolute quantification of cerebral blood flow in neurologically normal volunteers: dynamic-susceptibility contrast MRI-perfusion compared with computed tomography (CT)-perfusion. Magn Reson Med. 2009; 62(1):56–65. [PubMed: 19253361]
36. van Osch MJ, van der Grond J, Bakker CJ. Partial volume effects on arterial input functions: shape and amplitude distortions and their correction. J Magn Reson Imaging. 2005; 22(6):704–709. [PubMed: 16261570]
37. Helton KJ, et al. Arterial spin-labeled perfusion combined with segmentation techniques to evaluate cerebral blood flow in white and gray matter of children with sickle cell anemia. Pediatr Blood Cancer. 2009; 52(1):85–91. [PubMed: 18937311]
38. Han JS, et al. Measurement of cerebrovascular reactivity in pediatric patients with cerebral vasculopathy using blood oxygen level-dependent MRI. Stroke. 2011; 42(5):1261–1269. [PubMed: 21493907]

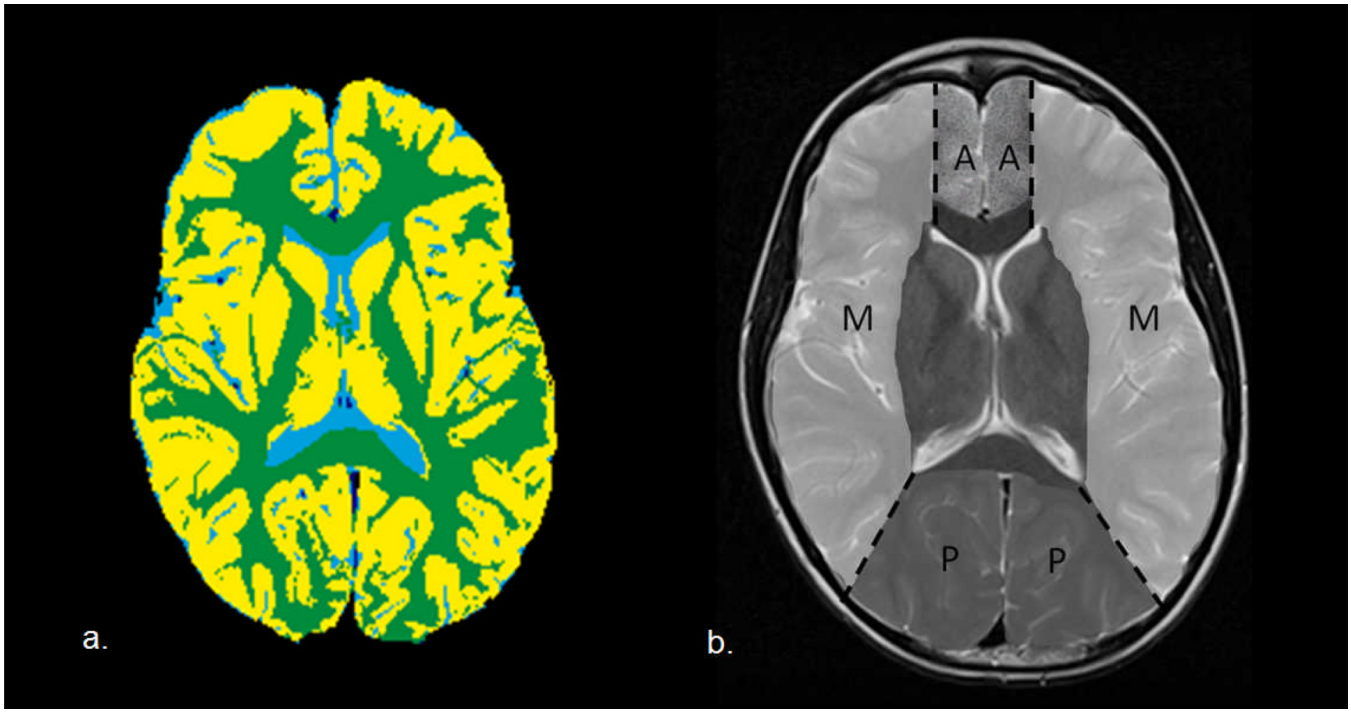


**Fig. 1.**
(a) Segmentation of gray matter and white matter on the index slice, and (b) illustration of regions of interest corresponding to the anterior cerebral artery (A), middle cerebral artery (M), and posterior cerebral artery (P) territories

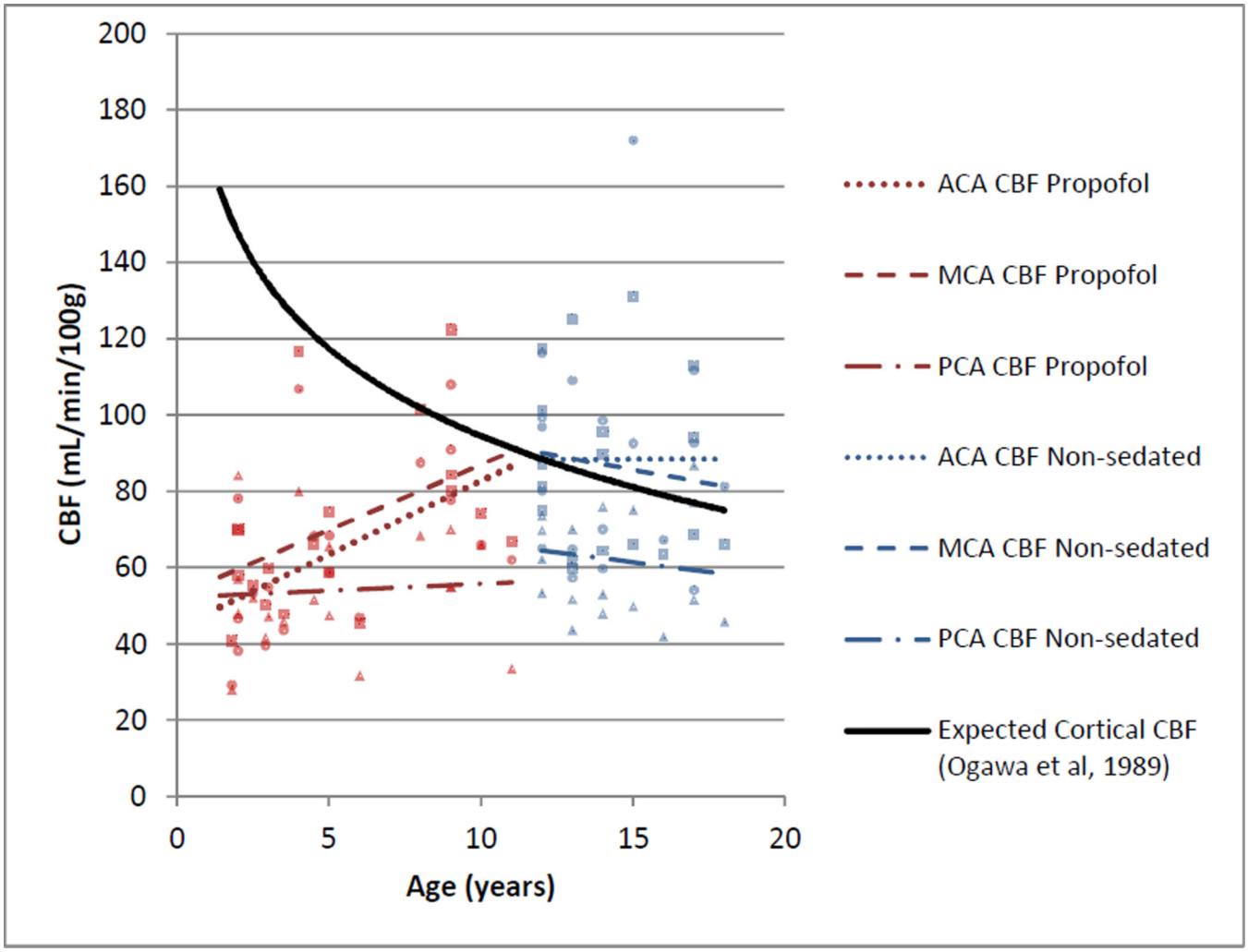


**Fig. 2.**

Visual comparison of trends of cortical GM CBF by age and vascular territory (ACA CBF, round data points; MCA CBF, square data points; and PCA CBF, triangle data points) in patients sedated with IV propofol and non-sedated patients for perfusion MRI, and age-related trends of GM CBF in non-sedated children by $^{133}$Xe nuclear medicine technique [11]

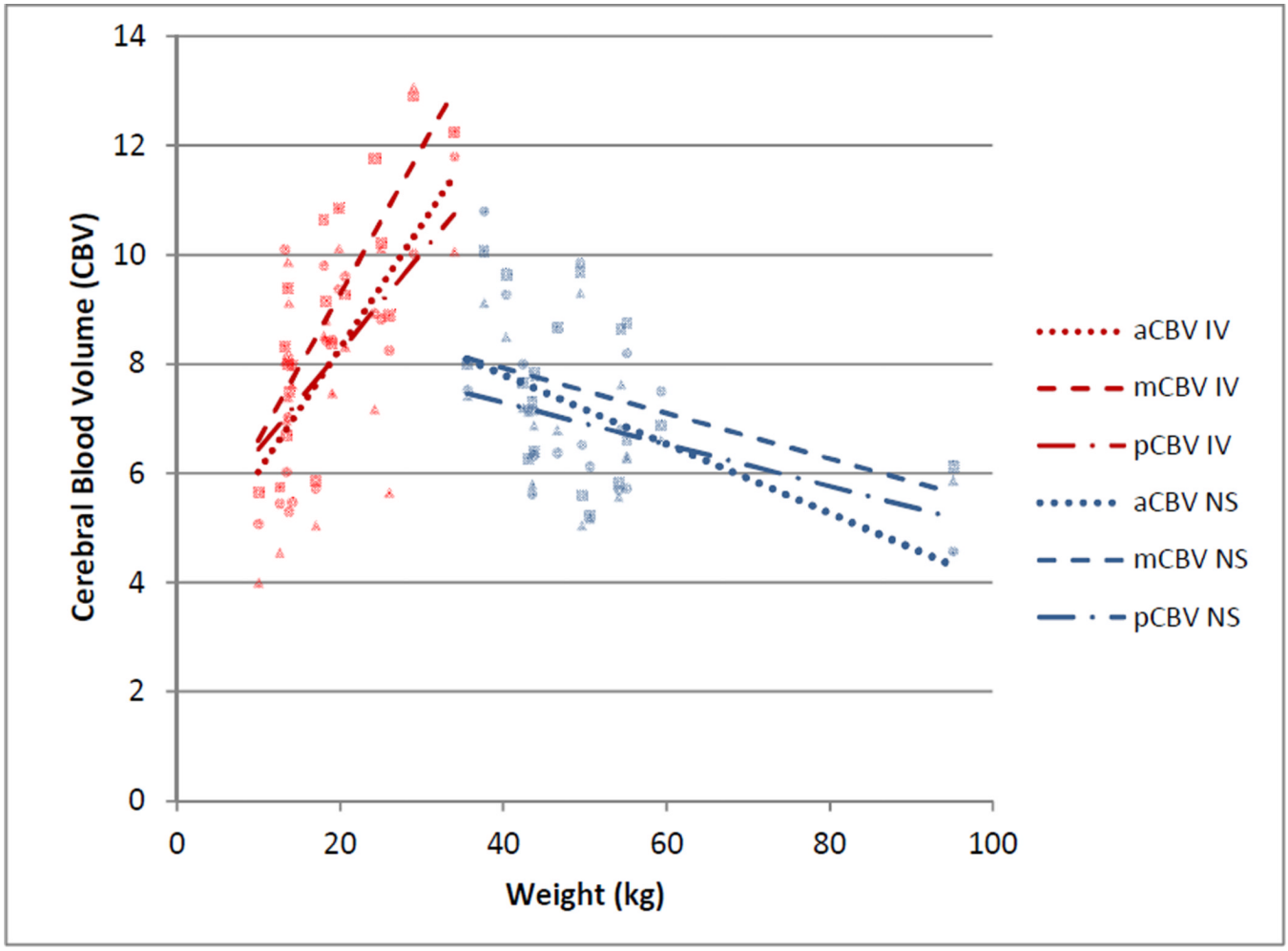


**Fig. 3.**

Cerebral blood volume by weight in the anterior cerebral artery (aCBV, round data points), middle cerebral artery (mCBV, square data points), and posterior cerebral artery (pCBV, triangle data points) territories by group (IV= propofol, NS=non-sedated). CBV increased with weight in patients receiving propofol

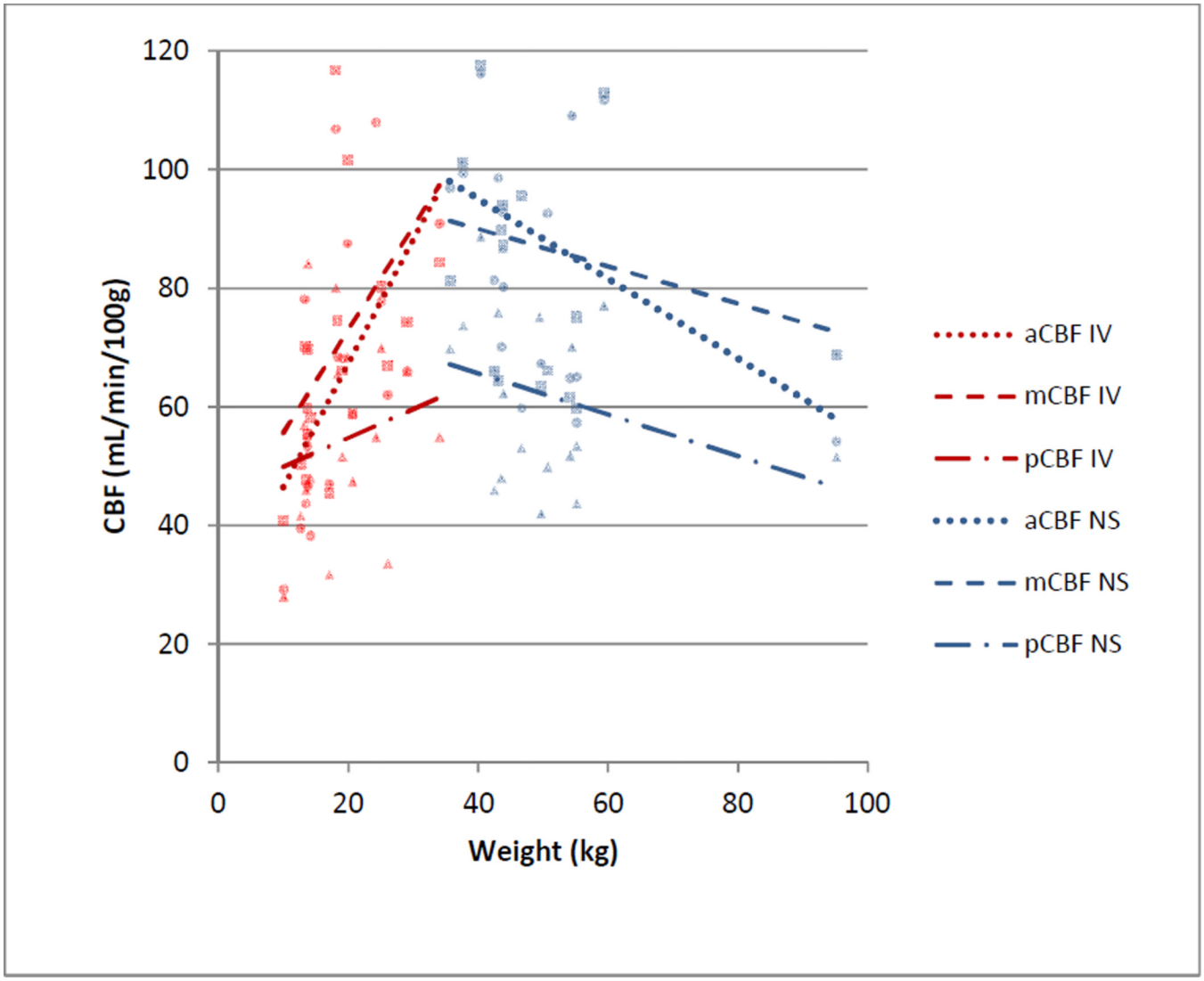


**Fig. 4.**

Cerebral blood flow (CBF) by weight in the anterior cerebral artery (aCBF, round data points), middle cerebral artery (mCBF, square data points), and posterior cerebral artery (pCBF, triangle data points) territories by group (IV= propofol, NS=non-sedated). CBF increased with weight in patients receiving propofol

**Table 1**

Comparison of CBF and CBV by vascular territory between patients sedated with IV propofol (IV) and nonsedated (NS) patients.

| | ACA | | MCA | | PCA | | |
|---|---|---|---|---|---|---|---|
| | **CBV** | **CBF** | **CBV** | **CBF** | **CBV** | **CBF** | **Age** |
| IV | **7.99** ± 1.99 | **64.51** ±22.58 | **8.92** ± 2.15 | **70.73** ±22.64 | **8.00** ± 2.23 | **54.12** ±15.44 | **5.27** ± 3.10 |
| NS | **7.18** ± 1.59 | **88.33** ±28.74 | **7.51** ± 1.50 | **86.78** ±23.20 | **6.91** ± 1.24 | **62.16** ±15.12 | **14.22** ± 2.05 |
| IV vs NS p= | 0.18 | **0.01** | **0.03** | **0.04** | 0.08 | 0.12 | **<0.0001** |

## Table 2

Correlation (r=Pearson correlation coefficient) of CBF and CBV with age and weight in children sedated with IV propofol. Correlations reaching statistical significance ($p<0.05$) are in bold.

| | Age | | Weight | |
|---|---|---|---|---|
| | r | p | r | p |
| **ACA CBV** | **0.56** | 0.01 | **0.73** | 0.0004 |
| **ACA CBF** | **0.53** | 0.02 | **0.59** | 0.0074 |
| **MCA CBV** | **0.67** | 0.002 | **0.80** | <0.0001 |
| **MCA CBF** | **0.47** | 0.04 | **0.49** | 0.03 |
| **PCA CBV** | 0.35 | 0.14 | **0.52** | 0.023 |
| **PCA CBF** | 0.07 | 0.77 | 0.20 | 0.41 |

## Table 3

Parameter estimate (regression coefficient). $R^2$, and p-value for the best-fit model of CBV and CBF by territory.

| | Weight | | |
|---|---|---|---|
| | **Estimate** | **p** | **$R^2$** |
| **ACA CBV** | 0.2261 | 0.0004 | 0.5308 |
| **ACA CBF** | 2.0882 | 0.0074 | 0.3522 |
| **MCA CBV** | 0.2681 | <0.0001 | 0.6400 |
| **MCA CBF** | 1.7372 | 0.0322 | 0.2424 |
| **PCA CBV** | 0.1800 | 0.0231 | 0.2683 |
| **PCA CBF** | 0.4872 | 0.4056 | 0.0410 |